Journal of Biomechanics 179 (2025) 112482

Contents lists available at ScienceDirect

Journal of Biomechanics

journal homepage: www.elsevier.com/locate/jbiomech

Short communication

Blood flow dynamics in the arterial and venous parts of the capillary

Viktor Dremin [a,b,c,*], Mikhail Volkov [d,e], Nikita Margaryants [f], Denis Myalitsin [e], Edik Rafailov [b], Andrey Dunaev [a]

[a] Research and Development Center of Biomedical Photonics, Orel State University, Orel, Russia
[b] Aston Institute of Photonic Technologies, Aston University, Birmingham, UK
[c] Optoelectronics and Measurement Techniques unit, University of Oulu, Oulu, Finland
[d] Scientific and Technological Center of Unique Instrumentation, Russian Academy of Sciences, Moscow, Russia
[e] ITMO University, Saint Petersburg, Russia
[f] Pavlov First Saint Petersburg State Medical University, Saint Petersburg, Russia

ARTICLE INFO

Keywords:
Capillaries
Blood flow
RBC velocity
Videocapillaroscopy
Oscillations
Wavelet coherence

ABSTRACT

Although there is currently sufficient information on various parameters of capillary blood flow, including the average values of blood velocity, there is no data on the dynamics of velocity and the mechanisms of its modulation in various parts of the capillary.

The main idea of this work is to develop a tool and image data processing to study the characteristics of the capillary blood flow dynamics. In this study, using the developed method of high-speed videocapillaroscopy, the red blood cells (RBC) velocities in the arterial and venous parts of the nailfold capillaries were compared and a time–frequency analysis of the dynamics of the velocity signals with the calculation of phase coherence was performed.

We indicated that the velocity in the arterial part is twice as high and that the ratio of velocities in the arterial and venous parts is stable regardless of the local velocity. This study also empirically confirms the similarity between the oscillations of blood flow in different parts of the capillary and the synchronization of the velocity phases. We believe that the determination of the absolute velocity characteristics of blood flow, together with the mechanisms of its regulation and the ratio of velocities in the arterial and venous parts, can act as a diagnostic approach.

1. Introduction

Most *in vivo* optical noninvasive diagnostic methods aimed at studying the blood flow of biological tissues deal with the microcirculatory vascular bed (Zharkikh et al., 2020; Makovik et al., 2018; Dremin et al., 2017). The microcirculatory bed includes arterioles, metarterioles, capillaries, and venules. The totality of these vessels is considered a functional unit of the vascular system, at the level of which blood performs its main function, the maintenance of cell metabolism. The structure of the vascular network is subordinated to the fulfillment of the main task — blood supply to all parts of the body at an optimal flow rate in the capillaries. Through the capillary wall, there is an exchange between blood and tissue.

Currently, the role of capillaries, their properties, and various parameters have been well studied (Guyton and Hall, 2006). They are the thinnest vessels with a diameter of 5–7 μm and a length of 0.5–1.1 mm. These vessels lie in intercellular spaces, in close contact with cells and tissues. The walls of the capillaries are formed by only one layer of endothelial cells, outside of which there is a thin basement membrane of connective tissue. The blood flow velocity in the capillaries varies depending on their location in the vascular system, but, generally, it remains relatively low and reaches units of mm/s. The blood velocity in the arterial and venous parts of the capillaries is also different. In the arterial part, where oxygen and nutrients are released to tissues, the velocity may be slightly higher. At the venous part, where carbon dioxide and other waste are collected, the velocity may decrease. In several previous studies, higher velocities have been shown in the arterial part of the human conjunctiva capillaries in comparison to the venous part (Koutsiaris et al., 2007, 2010). In addition, the “flattening” of the velocity pulse shape as the pulse proceeds in the rabbit mesentery capillaries has been reported in Ref. Koutsiaris and Pogiatzi (2003). This difference, along with the pressure gradient from the arterial to the venous endings, is necessary for the effective exchange of gases, nutrients, and waste products at the cellular level (Poole and Musch, 2023). The design of the capillary network ensures that there is enough time

* Corresponding author at: Aston Institute of Photonic Technologies, Aston University, Birmingham, UK.
E-mail address: v.dremin1@aston.ac.uk (V. Dremin).

https://doi.org/10.1016/j.jbiomech.2024.112482
Accepted 11 December 2024
Available online 19 December 2024

for this exchange despite the general high blood circulation velocity in the body. It is known that at rest in the arterial part of the capillaries, the hydrodynamic blood pressure reaches 30–35 mmHg, and in the venous part it decreases to 10–15 mmHg. Additionally, recent work has demonstrated changes in blood oxygen saturation in various parts of the capillaries. According to the study, the level of blood deoxygenation is 7.1% per hundred microns of length (Akons et al., 2017).

Although there is enough information on the average values of blood velocity in the capillaries, there is no data on the dynamics of velocity in various parts of the capillary. This study will present a comparison of blood flow rates in different parts of the capillary, as well as a time–frequency analysis of the dynamics of velocity signals with the calculation of phase coherence. This will allow us to study blood flow oscillations, as well as the synchronization of velocity phases.

2. Image acquisition and processing

In this work, we studied the blood flow in the nailfold capillaries. These capillaries have a thickness and density typical of peripheral tissues. The nailfold capillaries have a linear and arcade structure. Capillaries line up along the axis of the nail, forming parallel rows or arcades that follow the direction of growth of the nail plate. This structure helps to evenly supply the nailfold with blood. The study of blood flow dynamics was performed using the experimental high-speed videocapillaroscopy (VCS) technique developed earlier. This is a fairly popular technology for the direct study of blood flow in capillaries (Stavtsev et al., 2019; Yakimov et al., 2020; Lim et al., 2023). The high-speed VCS technique enables one to obtain detailed information about the red blood cells (RBCs) velocity into a capillary as well as a capillary net morphology. The nailfold area of the index finger of the hand was illuminated with a white LED. A 5X microscope objective with an aperture of 0.14 and a long-focus lens formed a capillary image. To restore the blood flow rate, a recording speed of at least 150 frames per second (FPS) is required. During the experiments, a high-speed CMOS camera was used to obtain video data. To solve the video frames stabilization problem, we used the algorithm based on the phase correlation principle (Karimov and Volkov, 2015). Thereafter, we applied the inter-frame image processing to evaluate the RBC velocity. The signals originated from the moving RBCs were compared with each other on the matter of mutual inter-frame shift. The shift value was assessed under the criterion of maximal correlation between each pairs of signals belong to adjacent video frames. The obtained values were averaged over all points of the central capillary line, yielding a stable estimation of the RBC velocity into a capillary. The detailed description of the system and algorithms for video frames processing is presented in Refs. Gurov et al. (2018, 2019), Dremin et al. (2019). The study was carried out on a 41-year-old male astronaut with excellent health status. The values of blood pressure and resting heart rate corresponded to the norm. The study was approved by the Ethics Committee of Orel State University.

First, an augmented Dickey–Fuller test was performed to confirm the nonstationarity of the original series. The time–frequency analysis of the obtained signals was performed using the continuous wavelet transform (CWT). The velocity signals were decomposed using CWT in the form (Bračič and Stefanovska, 1998):

$$W_x(s,\tau) = \frac{1}{\sqrt{s}} \int_{-\infty}^{\infty} x(t)\psi^* \left(\frac{t-\tau}{s}\right) dt, \tag{1}$$

where $x(t)$ is a target signal, τ is the time shift of the wavelet, s is the scaling factor, and the symbol * means complex conjugation. The decomposition was performed using the Morlet wavelet (Bračič and Stefanovska, 1998):

$$\psi(t) = \frac{1}{\sqrt[4]{\pi}} e^{2\pi i t} e^{-t^2/2}. \tag{2}$$

The Morlet wavelet is one of the most commonly used wavelets. This is the most reliable wavelet for time–frequency analysis of non-stationary time series data, particularly of biological nature.

The microvascular blood flow is subject to oscillations of different natures, which reflect the regulatory processes in the cardiovascular system. At present it is widely accepted that the frequency range from 0.005 to 2 Hz contains several intervals (Kvandal et al., 2006): cardiac (0.45–2 Hz), respiratory (0.2–0.45 Hz), myogenic (0.05–0.15 Hz), neurogenic (0.02–0.05 Hz) and endothelial (0.005–0.02 Hz). In our study, oscillations in the frequency interval of neurogenic and endothelial activity (0.005–0.05 Hz) were not analyzed since correct evaluation of such slow oscillations requires longer signal registration times.

The time–frequency comparison of two nonstationary signals can be provided involving wavelet-based coherence. The wavelet coherence allows one to calculate the local correlation of two functions $x(t)$ and $y(t)$ with wavelet transforms $W^x(s,\tau)$ and $W^y(s,\tau)$ in the time–frequency domain (Torrence and Webster, 1999; Grinsted et al., 2004). This value is calculated as the absolute value squared of the smoothed cross-wavelet spectrum, normalized by the smoothed wavelet power spectra:

$$R^2(s,\tau) = \frac{\left|H\left(s^{-1}W^{xy}(s,\tau)\right)\right|^2}{H\left(s^{-1}|W^x(s,\tau)|^2\right)\cdot H\left(s^{-1}|W^y(s,\tau)|^2\right)}, \tag{3}$$

where $W^{xy}(s,\tau) = W^x(s,\tau)W^{y*}(s,\tau)$ is a cross-wavelet spectrum, H is a smoothing operator. The smoothing in Eq. (3) is based on a weighted moving average in both the time and scale directions as described in detail by Torrence and Compo (1998). The smoothing assists in removing the singularities in wavelet power spectra and improves the reliability of calculations.

Wavelet coherence also makes it possible to study the phase dependence between two time series. This shows whether one signal is ahead of another or behind it and how big this time difference is. The phase difference of the corresponding oscillations is given by:

$$\phi^{xy}(s,\tau) = \arctan \frac{\Im(W^{xy}(s,\tau))}{\Re(W^{xy}(s,\tau))}. \tag{4}$$

The degree of correlation between the phases of the analyzed signals can be estimated by calculating the phase coherence function (Bandrivskyy et al., 2004):

$$C_\phi = \sqrt{\langle\cos\Delta\phi(s,\tau)\rangle^2 + \langle\sin\Delta\phi(s,\tau)\rangle^2}, \tag{5}$$

where $\Delta\phi(s,\tau) = \phi^x(s,\tau) - \phi^y(s,\tau)$, is the instantaneous phase of $x(t)$ and $y(t)$ signals. If the phase difference is almost constant, the phase coherence tends to become 1, if it $\Delta\phi(s,\tau)$ is random, then C_ϕ tends to zero. Thus, the phase difference between the two oscillations is allowed provided that it remains constant throughout the observation time.

The significance of the correlation is verified by constructing the surrogate data. For surrogate generation, we employed the method of amplitude-adjusted Fourier transform (AAFT) (Lancaster et al., 2018). The AAFT produces surrogates with original values retained in the time series but rearranged in a way that largely preserves the spectrum while destroying temporal information. We provided 100 pairs of surrogate data for each pair of experimental signal samples. Significance levels were calculated as the 95th percentile of surrogates.

3. Results and discussion

Fig. 1a shows a full-frame panorama of the nailfold capillaries at a recording rate of 50 FPS. This frame rate is not sufficient to restore velocity in all capillaries but is suitable for studying the morphology of the microcirculatory bed in a large area of interest.

The local velocity of capillary blood flow at a recording rate of 150 FPS is shown in Fig. 1b. The map of local velocities at each moment of time is shown in Fig. 1c. The local flow velocity is represented in the orange scale in dependence on time (in the horizontal axis), whereas the vertical position corresponds to different points along a capillary

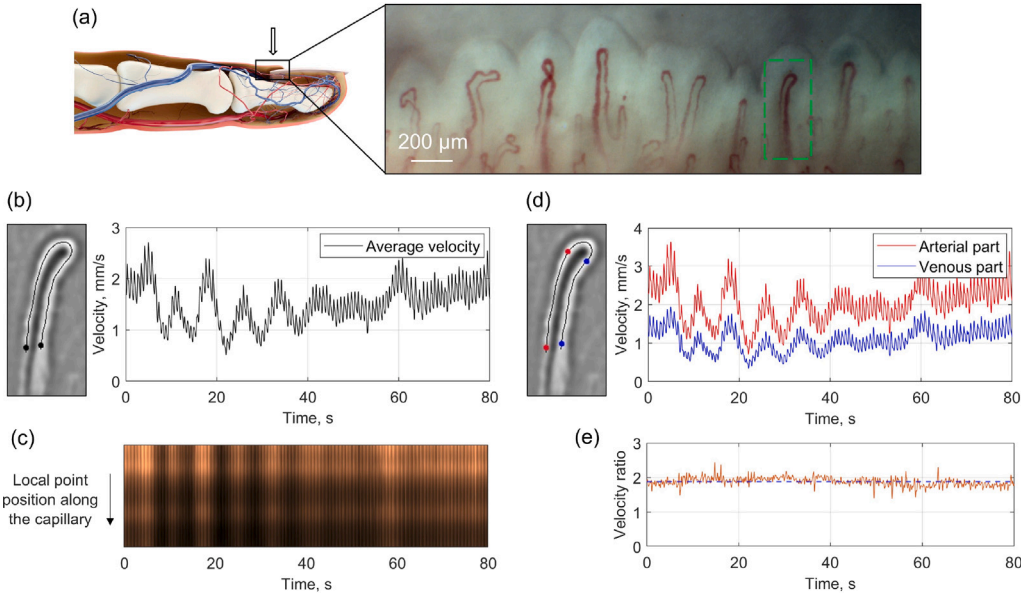

Fig. 1. High-speed videocapillaroscopy of the nailfold. (a) The panoramic image of capillaries obtained for the nailfold of the finger. The analyzed capillary is highlighted with a green dashed rectangle. (b) Measurement of RBC velocity in the entire capillary and (c) map corresponding to the velocity averaged over all points along the capillary and associated with local capillary points. (d) Measurement of blood flow velocity in the arterial and venous parts of the capillary and (e) velocity ratio. The video of this experiment is available as Video 1 (MP4, 963KB) and Video 2 (MP4, 1MB).

central line. It can be seen that in 80 s the velocity varies between 0.6–2.6 mm/s. We can also use the graph to determine a heart rate. In the first 60 s, it is 77. However, the values shown represent the average velocity in the capillary loop. Fig. 1d shows a comparison of velocities in the arterial and venous parts of the capillary. As can be seen, the velocity in the arterial part is twice as high, but the time changes have a similarity, and the ratio of velocities in the arterial and venous parts is stable regardless of the local velocity at each moment of time (Fig. 1e).

Fig. 2 corresponds to the CWT representation. Figs. 2a,b show the CWT scalogram charts represented as a gradient colored map with the distribution of the wavelet power of the signal in the time–frequency domain. The blue regions relate to the lowest power, while the red ones correspond to the highest values. Mean time-averaged normalized spectra are shown in Fig. 2c.

The similarity of the changes in the temporal dynamics of blood flow in the two parts of the capillary corresponds to the similarity of their CWT. Calculating the wavelet coherence and phase coherence in correspondence with Eqs. (3) and (5) confirms the similarity of signals and allows one to reveal their relationships and represent them in numerical form. In Fig. 2d, the arrows show the phase lag of one signal relative to another. Phase arrows are shown only where the coherence is greater than or equal to 0.5. The direction of the arrows corresponds to the value of the phase lag. The arrows pointing to the right or left show two in-phase or anti-phase signals, respectively. The vertical arrow indicates $\pi/2$ or quarter-cycle phase lag. In our case, we see the common-mode behavior of signals in almost the entire target frequency range.

Figs. 2d,e illustrate an area of significant consistency throughout the data collection period over a wide frequency range from 0.1 to 2 Hz. Thus, we see a high coherence of signals in the cardiac, respiratory, and myogenic bands. Although our recordings did not allow us to reliably analyze neurogenic and endothelial rhythms, it is reasonable to assume high coherence for them as well. To confirm the significance of our findings, we show in Fig. 2e the average coherence and the 95th percentile calculated for 100 surrogates. The surrogate example is shown in Fig. 2f.

The flow rate in the vessels is one of the most important parameters of the circulatory system. It is determined by the main task of the system — to ensure adequate exchange between blood and tissues. This process is critical for maintaining homeostasis in the body. The relatively low diffusion rate of gases and basic chemicals through the walls of capillaries and cells dictates the need for a certain flow rate in the capillaries. Therefore, maintaining an optimal flow rate is the most important task of the control system. This rate is regulated by various mechanisms and understanding these physiological patterns is extremely important.

The blood flow rate in capillaries strongly depends on many factors, including the diameter of the capillaries, the total resistance of the blood vessels, blood pressure and the state of the vascular system. More specifically, the observed decrease in the RBC velocity in the venous part of the capillary can occur for a number of reasons, including compliance with the law of conservation of mass, in which an increase in the cross-sectional area of the capillary leads to a decrease in the blood flow velocity, as well as filtration and reabsorption processes, which can lead to a change in the circulating volume in the venous part.

The study demonstrates the physiological importance of capillary blood flow regulation, highlighting how differences in velocity facilitate efficient nutrient and oxygen exchange in the arterial region and waste removal in the venous region. A time–frequency analysis revealed that oscillations in blood flow within the arterial and venous segments of capillaries show high coherence, particularly in cardiac, respiratory, and myogenic frequency bands. Given the volunteer status, we assume that this coordinated control suggests a mechanism of blood flow regulation indicative of healthy vascular function, offering diagnostic potential for identifying vascular abnormalities. Disruptions in phase coherence may signal pathological changes. Furthermore, the stability of the velocity ratio between arterial and venous parts, independent of absolute local velocity, could serve as a diagnostic marker. Deviations in this ratio might indicate vascular changes, such as capillary thickening or stasis, commonly associated with specific diseases. Conditions like diabetes, hypertension, and cardiovascular diseases often manifest microcirculatory abnormalities early on, even before other symptoms appear. By analyzing capillary blood flow patterns and phase coherence, clinicians may potentially identify patients at risk sooner, enabling timely interventions. However, this requires additional clinical studies.

The velocity ratio can also characterize the ratio of the diameters of the venous and arterial parts of the capillary. Using the law of

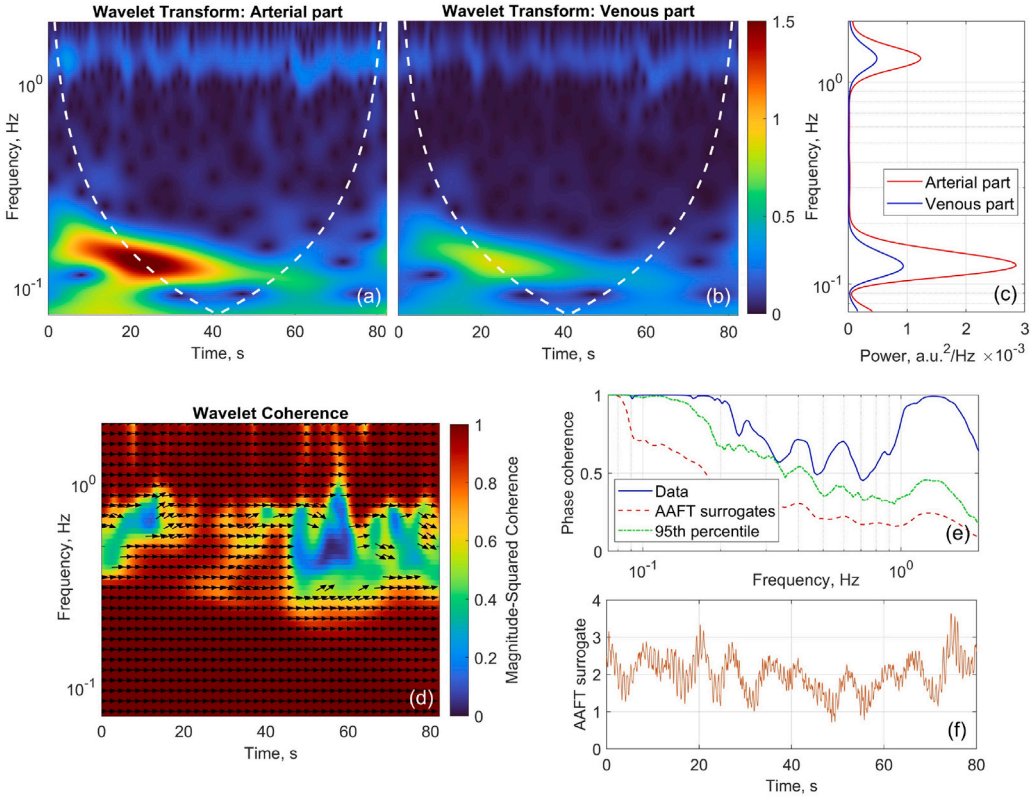

Fig. 2. The time–frequency analysis. (a,b) CWT representation of the RBC velocity in the arterial and venous parts of the capillary, respectively. The white dashed line shows the cone of influence where edge effects become significant at different frequencies. The areas outside or overlapping the cone of influence should be interpreted with caution. (c) Mean time-averaged normalized spectra. (d) Wavelet coherence between velocities in different parts of the capillary. The arrows show the phase lag of the signal from the arterial part with respect to the venous part. (e) Wavelet phase coherence compared with the significance levels of the surrogate types shown, calculated as the 95th percentile of 100 surrogates. (f) An example of an AAFT surrogate. (For interpretation of the references to color in this figure legend, the reader is referred to the web version of this article.)

conservation of mass, we can approximately estimate the ratio of the diameters of the capillary parts using calculated velocity values. For the presented experiment, this value was 1.41, and calculated directly from grayscale images was 1.49. Given that we measured the RBC velocity and not the blood flow velocity, the observed difference can be potentially adjusted for the Fahraeus effect (Albrecht et al., 1979).

4. Conclusion

In the present study, the correlation between the dynamics of blood flow in the arterial and venous parts of the capillary was analyzed using the calculation of wavelet coherence. We showed that blood flow oscillations in cardiac, respiratory and myogenic frequency intervals might have high and reliable phase coherence for different parts of the capillary. Meanwhile, blood flow velocities are in-phase. It is important to clarify that the capillary of a completely healthy volunteer was examined. We believe that with the thickening of capillaries or stagnant processes, the phase shift may increase.

Thus, although one subject was involved in the study, with this work we demonstrate an approach that expands our basic understanding of the capillary bed, and can also be applied in various clinical applications.

CRediT authorship contribution statement

Viktor Dremin: Writing – original draft, Software, Project administration, Formal analysis, Data curation, Conceptualization. **Mikhail Volkov:** Writing – review & editing, Software, Investigation, Formal analysis, Data curation, Conceptualization. **Nikita Margaryants:** Writing – review & editing, Investigation, Formal analysis, Conceptualization. **Denis Myalitsin:** Writing – review & editing, Software, Formal analysis. **Edik Rafailov:** Writing – review & editing, Conceptualization. **Andrey Dunaev:** Writing – review & editing, Investigation, Conceptualization.

Declaration of competing interest

The authors declare that they have no known competing financial interests or personal relationships that could have appeared to influence the work reported in this paper.

Acknowledgments

VD acknowledges the support of the Russian Science Foundation, Russia (grant No. 22-75-10088, development of data analysis algorithms) and the Academy of Finland, Finland (visiting grant No. 347876). The authors are very grateful to Russian astronaut Alexander Misurkin for participation in the experiment.

Appendix A. Supplementary data

Supplementary material related to this article can be found online at https://doi.org/10.1016/j.jbiomech.2024.112482.

Data availability

Data underlying the results may be obtained from the authors upon reasonable request.

References

Akons, K., Dann, E.J., Yelin, D., 2017. Measuring blood oxygen saturation along a capillary vessel in human. Biomed. Opt. Expr. 8 (11), 5342–5348.

Albrecht, K., Gaehtgens, P., Pries, A., Heuser, M., 1979. The fahraeus effect in narrow capillaries (i.d. 3.3 to 11.0 μm). Microvasc. Res. 18 (1), 33–47.

Bandrivskyy, A., Bernjak, A., McClintock, P., Stefanovska, A., 2004. Wavelet phase coherence analysis: Application to skin temperature and blood flow. Cardiovasc. Eng. 4 (1), 89–93.

Bračič, M., Stefanovska, A., 1998. Wavelet-based analysis of human blood-flow dynamics. Bull. Math. Biol. 60 (5), 919–935.

Dremin, V., Kozlov, I., Volkov, M., Margaryants, N., Potemkin, A., Zherebtsov, E., Dunaev, A., Gurov, I., 2019. Dynamic evaluation of blood flow microcirculation by combined use of the laser Doppler flowmetry and high-speed videocapillaroscopy methods. J. Biophotonics 12 (6), e201800317.

Dremin, V.V., Zherebtsov, E.A., Makovik, I.N., Kozlov, I.O., Sidorov, V.V., Krupatkin, A.I., Dunaev, A.V., Rafailov, I.E., Litvinova, K.S., Sokolovski, S.G., Rafailov, E.U., 2017. Laser Doppler flowmetry in blood and lymph monitoring, technical aspects and analysis. Proc. SPIE 10063, 1006303.

Grinsted, A., Moore, J.C., Jevrejeva, S., 2004. Application of the cross wavelet transform and wavelet coherence to geophysical time series. Nonlinear Process. Geophys. 11, 561–566.

Gurov, I., Volkov, M., Margaryants, N., Pimenov, A., Potemkin, A., 2018. High-speed video capillaroscopy method for imaging and evaluation of moving red blood cells. Opt. Lasers Eng. 104, 244–251.

Gurov, I., Volkov, M., Margaryants, N., Potemkin, A., 2019. Method of bringing locally varying images into coincidence in video capillaroscopy. J. Opt. Technol. 86, 774–780.

Guyton, A.C., Hall, J.E., 2006. Textbook of Medical Physiology, Eleventh ed. Elsevier.

Karimov, K.A., Volkov, M.V., 2015. The phase correlation algorithm for stabilization of capillary blood flow video frames. Proc. SPIE 9528, 952810.

Koutsiaris, A.G., Pogiatzi, A., 2003. Velocity pulse measurements in the mesenteric arterioles of rabbits. Physiol. Meas. 25 (1), 15.

Koutsiaris, A.G., Tachmitzi, S.V., Batis, N., Kotoula, M.G., Karabatsas, C.H., Tsironi, E., Chatzoulis, D.Z., 2007. Volume flow and wall shear stress quantification in the human conjunctival capillaries and post-capillary venules in vivo. Biorheology 44, 375–386.

Koutsiaris, A.G., Tachmitzi, S.V., Papavasileiou, P., Batis, N., Kotoula, M.G., Giannoukas, A.D., Tsironi, E., 2010. Blood velocity pulse quantification in the human conjunctival pre-capillary arterioles. Microvasc. Res. 80 (2), 202–208.

Kvandal, P., Landsverk, S.A., Bernjak, A., Stefanovska, A., Kvernmo, H.D., Kirkebøen, K.A., 2006. Low-frequency oscillations of the laser Doppler perfusion signal in human skin. Microvasc. Res. 72 (3), 120–127.

Lancaster, G., Iatsenko, D., Pidde, A., Ticcinelli, V., Stefanovska, A., 2018. Surrogate data for hypothesis testing of physical systems. Phys. Rep. 748, 1–60.

Lim, M., Setjiadi, D., Dobbin, S., Lang, N., Delles, C., Connelly, P., 2023. Nailfold video-capillaroscopy in the study of cardiovascular disease: a systematic review. Blood Press. Monit. 28, 24–32.

Makovik, I.N., Dunaev, A.V., Dremin, V.V., Krupatkin, A.I., Sidorov, V.V., Khakhicheva, L.S., Muradyan, V.F., Pilipenko, O.V., Rafailov, I.E., Litvinova, K.S., 2018. Detection of angiospastic disorders in the microcirculatory bed using laser diagnostics technologies. J. Innov. Opt. Health Sci. 11 (01), 1750016.

Poole, D.C., Musch, T.I., 2023. Capillary-mitochondrial oxygen transport in muscle: Paradigm shifts. Function 4 (3), zqad013.

Stavtsev, D.D., Volkov, M.V., Margaryants, N.B., Potemkin, A.V., Dremin, V.V., Kozlov, I.O., Makovik, I.N., Zherebtsov, E.A., Dunaev, A.V., 2019. Investigation of blood microcirculation parameters in patients with rheumatic diseases by videocapillaroscopy and laser Doppler flowmetry during cold pressor test. Proc. SPIE 11065, 110650T.

Torrence, C., Compo, G.P., 1998. A practical guide to wavelet analysis. Bull. Am. Meteorol. Soc. 79, 61–78.

Torrence, C., Webster, P.J., 1999. Interdecadal changes in the ENSO–monsoon system. J. Clim. 12 (8), 2679–2690.

Yakimov, B., Gurfinkel, Y., Davydov, D., Allenova, A., Budylin, G., Vasiliev, V., Soldatova, V., Kamalov, A., Matskeplishvili, S., Priezzhev, A., Shirshin, E., 2020. Pericapillary edema assessment by means of the nailfold capillaroscopy and laser scanning microscopy. Diagnostics 10 (12), 1107.

Zharkikh, E., Dremin, V., Zherebtsov, E., Dunaev, A., Meglinski, I., 2020. Biophotonics methods for functional monitoring of complications of diabetes mellitus. J. Biophotonics 13, 202000203.